# An EM-based Identification Algorithm for a Class of Hybrid Systems with Application to Power Electronics

R. P. Aguilera[a]*, B. I. Godoy[a], J. C. Agüero[a], G. C. Goodwin[a], and J. I. Yuz[b]
[a] *The University of Newcastle, Newcastle, Australia*;
[b] *Universidad Técnica Federico Santa María, Valparaíso, Chile.*

December 15, 2013

**Abstract**

In this paper we present an identification algorithm for a class of continuous-time hybrid systems. In such systems, both continuous-time and discrete-time dynamics are involved. We apply the Expectation-Maximization algorithm to obtain the maximum likelihood estimate of the parameters of a discrete-time model expressed in incremental form. The main advantage of this approach is that the continuous-time parameters can directly be recovered. The technique is particularly well suited to fast sampling rates. As an application, we focus on a standard identification problem in power electronics. In this field, our proposed algorithm is of importance since accurate modelling of power converters is required in high performance applications and for fault diagnosis. As an illustrative example, and to verify the performance of our proposed algorithm, we apply our results to a flying capacitor multicell converter.

## 1 Introduction

Hybrid systems present continuous-time dynamics subject to changes in regime. These changes in regime belong to a finite or countable set. Thus, in such systems, both continuous-time and discrete-time dynamics are involved. Hybrid systems have been a topic of recurrent interest in the areas of econometrics, biological systems, engineering, etc, see e.g., [1, 2].

In the area of power electronics, hybrid systems have been used extensively to model power converters and electrical drives [3]. Power converters have played an important role in the expansion of the use of electrical power in a wide variety of applications, including mining, medicine, transportation, and renewable energy [4]. Most applications are critical processes, where energy conversion must be carried out with high power quality (i.e., reduced harmonic pollution), and high reliability [5].

In terms of power quality, multilevel converters have emerged as a promising alternative to traditional two-level converters [6]. Multilevel topologies are able to operate at much higher power levels. They also provide output voltages and currents with lower distortion than their two-level

*Corresponding author. Email: raguilera@ieee.org. This work is partially supported by the Australian Research Council through Discovery Projects and by the Chilean Research Council (CONICYT) through grants Anillo ACT-53 and FONDECYT 1130861.

counterparts. They employ series connected switching devices, and an assortment of passive storage elements, to produce multiple distinct voltage levels between which the converter output can be switched. This allows the synthesis of switched waveforms with staircase envelopes that contain very low levels of harmonic distortion. Since multilevel topologies have more components than the corresponding two-level converter counterparts, they have a higher probability to present internal faults. Thus, it is important to monitor the internal components in order to evaluate the health of the devices.

In the engineering literature, several identification algorithms have been proposed for hybrid systems. Most of these works are based on using a linear regression approach, see e.g. [7, 8, 9, 10, 1]. In [11], a system identification strategy for stochastic hybrid systems is presented. However, the proposed methodology does not consider model uncertainties and the measurement covariance is assumed to be known.

In this paper, we propose an identification algorithm for a class of hybrid systems based on the preliminary work describe earlier in [12] . The proposed algorithm is based on maximum-likelihood estimation. The system is parameterised in the, so called, delta (or incremental) form [13]. This kind of system modelling differs from the usual practice of using shift-operator models. Incremental models are obtained by simply reparameterising the discrete-time model. The use of this kind of model gives a framework which allows one to unify discrete- and continuous-time results in estimation and control when fast sampling rates are used [14].

In this paper, we exploit these properties by applying the Expectation-Maximisation (EM) algorithm to maximise the likelihood function associated with the incremental model to obtain estimates of the hybrid model parameters. The EM algorithm is a recursive two step procedure. In the first step, a function of the state sequence estimate is obtained assuming that the parameters are known (E-step). In the second step, the function obtained in the E-step is maximised with respect to the parameters to obtain a new estimate (M-step). This yields a new parameter estimate to be used in the next iteration of the algorithm [15]. Our identification proposal does not require a priori knowledge of the process and measurement noise covariances since they are also estimated. We apply the EM algorithm to the problem of internal identification of power converters. This allows one to monitor the health condition of such hybrid systems.

As an illustrative example, we apply the proposed identification algorithm to estimate the internal capacitance values of a multicell power converter.

# 2 Problem Set up

## 2.1 Continuous-time model

Consider the following general continuous hybrid system described by state-space matrices. Each of the state-space matrices is parametrized by a common parameter vector $\theta$, that is:

$$\begin{aligned} \dot{x}(t) &= A^c_{\sigma(t)}(\theta)x(t) + B^c_{\sigma(t)}(\theta)u(t) + \dot{w}(t) \\ \frac{dz(t)}{dt} &= C^c_{\sigma(t)}(\theta)x(t) + D^c_{\sigma(t)}(\theta)u(t) + \dot{v}(t) \end{aligned} \tag{1}$$

where $x(t) \in \mathbb{R}^n$, $z(t) \in \mathbb{R}^{n_y}$, $u(t) \in R^{n_u}$, $\dot{w}(t) \in \mathbb{R}^n$, $\dot{v}(t) \in \mathbb{R}^{n_y}$. Also, $\sigma(t)$ is an indicator of the system configuration. Here we assume $\sigma(t)$ can take one of $m$ values.

Additionally, the process noise $\dot{w}(t)$ and the measurement noise $\dot{v}(t)$ are the *formal* derivatives of Wiener processes $w(t)$ and $v(t)$, respectively, with incremental covariance:

$$\mathbb{E}\{\begin{bmatrix}\dot{w}(t)\\ \dot{v}(t)\end{bmatrix}\begin{bmatrix}\dot{w}(s) & \dot{v}(s)\end{bmatrix}\} = \begin{bmatrix}Q^c & 0\\ 0 & R^c\end{bmatrix}\delta(t-s). \tag{2}$$

**Remark 1** *A key observation in the continuous-time noise model in* (1)-(2)*, is that the matrices* $Q^c$ *and* $R^c$ *correspond to* spectral densities *of the noise processes [13]. In fact,* continuous-time white noise *(CTWN) processes have infinite variance [16]. They offer and ideal description of broadband stochastic disturbances in continuous-time.*

Such processes are usually referred to as CTWN. Notice that any continuous-time stochastic process with independent increments and finite second moment is necessarily a Gaussian process provided that it is Gaussian for some $t_0$ in the time interval of interest, see e.g. [17, p.28].

The matrices $A^c_{\sigma(t)}(\theta)$, $B^c_{\sigma(t)}(\theta)$, $C^c_{\sigma(t)}(\theta)$, $D^c_{\sigma(t)}(\theta)$ belong to a finite set $\mathcal{A}$, $\mathcal{B}$, $\mathcal{C}$, $\mathcal{D}$ respectively. These sets are described as:

$$\mathcal{A} = \{A^c_1(\theta), \ldots, A^c_m(\theta)\}, \quad \mathcal{B} = \{B^c_1(\theta), \ldots, B^c_m(\theta)\}, \tag{3}$$
$$\mathcal{C} = \{C^c_1(\theta), \ldots, C^c_m(\theta)\}, \quad \mathcal{D} = \{D^c_1(\theta), \ldots, D^c_m(\theta)\}, \tag{4}$$

where $A^c_i(\theta), B^c_i(\theta)$, $C^c_i(\theta)$, $D^c_i(\theta)$ $i = 1, \ldots, m$ is the result of (3) considering different values for $\sigma_{(t)}$.

Since the system matrices take different values, depending on the value for $\sigma_{(t)}$, the problem is a switched hybrid system. The goal is to estimate the parameter $\theta$. Notice that $\theta$ is a common parameter to all possible state-space matrices under different configuration scenarios.

This class of hybrid system encompasses several power converter topologies, e.g., DC-DC buck converter, DC-DC boost converter, active-front-end rectifier, and multicell converter, see e.g. [18, 19, 20, 21]. In Section 4, we illustrate the ideas for the specific problem of identification for a multicell converter.

### 2.2 Sampled-data model

We assume that the output samples of the system described in (1)-(2) are obtained using a constant sampling period

$$\Delta = t_{k+1} - t_k > 0 \quad ; \forall k \in \mathbb{N}. \tag{5}$$

A key point in this work is that we assume that the switching elements remain constant during each sampling period, $\Delta$, i.e.,

$$\sigma(t) = \sigma_k \in \{1, \ldots, m\} \quad ; t_k \leq t < t_{k+1}. \tag{6}$$

In this case, the hybrid model presented in (1) can be viewed as a time-varying linear system.

The sampling process of the system output must be dealt with carefully. From (1), we see that the output has a *pure CTWN component*. Instantaneous sampling of this output would lead to a sequence having infinite variance. We thus need to employ an anti-aliasing filter prior to sampling.

We will use an *integrate and reset* filter (IRF) at the system output before instantaneous sampling [13]:

$$\begin{aligned}\bar{y}(t_{k+1}) &= \frac{1}{t_{k+1}-t_k}\int_{t_k}^{t_{k+1}} \frac{dz_\tau}{d\tau} = \frac{1}{\Delta}\int_{t_k}^{t_{k+1}} dz(\tau) \\ &= \frac{z(t_{k+1})-z(t_k)}{\Delta}.\end{aligned} \tag{7}$$

Under these conditions, the samples can be described as follows:

**Lemma 1** *Consider the continuous-time state-space model* (1)*, where the system mode,* $\sigma(t)$*, is constant during each sampling period as per* (6) *and the output is sampled after the IRF presented in* (7)*. Then, the following incremental discrete-time model has the same second order output properties as the sampled output of the continuous-time system*[1]*:*

$$\begin{aligned}dx^+ &= A^\delta_{\sigma_k} x_k \Delta + B^\delta_{\sigma_k}\Delta + dw^+_k \\ \bar{y}_{k+1}\Delta_k = dz^+_k &= C^\delta_{\sigma_k} x_k \Delta + D^\delta_{\sigma_k}\Delta + dv^+_k,\end{aligned} \tag{8}$$

*where the increment is defined as,* $df^+_k = f_{k+1} - f_k$*. The matrices are given by (see e.g. [13, chap.6])*

$$A^\delta_{\sigma_k} = \frac{e^{A^c_{\sigma_k}\Delta} - I}{\Delta}, \quad B^\delta_{\sigma_k} = \left[\frac{1}{\Delta}\int_0^\Delta e^{A^c_{\sigma_k}\eta} d\eta\right] B^c_{\sigma_k} \tag{9}$$

$$C^\delta_{\sigma_k} = C^c_{\sigma_k}\left[\frac{1}{\Delta}\int_0^\Delta e^{A^c_{\sigma_k}\eta} d\eta\right] \tag{10}$$

$$D^\delta_{\sigma_k} = D^c_{\sigma_k} + C^c_{\sigma_k}\left[\frac{1}{\Delta}\int_0^\Delta\int_0^\epsilon e^{A^c_{\sigma_k}\eta} d\eta d\epsilon\right] B^c_{\sigma_k}, \tag{11}$$

*and the covariance structure of the noise vector is*

$$\mathbb{E}\left\{\begin{bmatrix} dw^+_l \\ dv^+_l\end{bmatrix}\begin{bmatrix} dw^+_k \\ dv^+_k\end{bmatrix}\right\} = \begin{bmatrix} Q^\delta_{\sigma_k} & S^\delta_{\sigma_k} \\ [S^\delta_{\sigma_k}]^T & R^\delta_{\sigma_k}\end{bmatrix}\Delta\delta_K(l-k) \tag{12}$$

*where* $\delta_K$ *is the Kronecker delta and*

$$\begin{bmatrix} Q^\delta_{\sigma_k} & S^\delta_{\sigma_k} \\ [S^\delta_{\sigma_k}]^T & R^\delta_{\sigma_k}\end{bmatrix} = \frac{1}{\Delta}\int_0^\Delta \begin{bmatrix} e^{A^c_{\sigma_k}\eta} & 0 \\ C^c_{\sigma_k}\int_0^\eta e^{A^c_{\sigma_k}\epsilon} d\epsilon & I\end{bmatrix}\begin{bmatrix} Q^c & 0 \\ 0 & R^c\end{bmatrix}\begin{bmatrix} e^{A^c_{\sigma_k}\eta} & 0 \\ C^c_{\sigma_k}\int_0^\eta e^{A^c_{\sigma_k}\epsilon} d\epsilon & I\end{bmatrix} d\eta. \tag{13}$$

**Proof** The proof of this lemma is similar to that of Lemma 1 in [12]. ■

**Remark 2** *The above model has been expressed in incremental form. An equivalent shift operator model is*

$$\begin{aligned}x_{k+1} &= A^q_{\sigma_k} x_k + B^q_{\sigma_k} u_k + w_k, \\ y_k &= C^q_{\sigma_k} x_k + D^q_{\sigma_k} u_k + v_k,\end{aligned} \tag{14}$$

[1]For simplicity of notation, we will omit the dependency on the parameter vector $\theta$ for the state-space matrices.

*where* $x_k \in \mathbb{R}^n$, $y_k \in \mathbb{R}^{n_y}$, *and* $u \in \mathbb{R}^{n_u}$, $\begin{bmatrix} w_k \\ v_k \end{bmatrix} \sim \begin{bmatrix} Q^q & S^q \\ [S^q]^T & R^q \end{bmatrix}$, $Q^q \in \mathbb{R}^{n\times n}$, $R^q \in \mathbb{R}^{n_y \times n_y}$, $S^q \in \mathbb{R}^{n\times n_y}$. *The expressions for* $A^q_{\sigma_k}$, $B^q_{\sigma_k}$, $C^q_{\sigma_k}$, *and* $D^q_{\sigma_k}$, $Q^q$, $R^q$, *and* $S^q$ *are given by:*

$$A^q_{\sigma_k} = I + \Delta A^\delta_{\sigma_k}, \qquad B^q_{\sigma_k} = \Delta B^\delta_{\sigma_k}, \qquad C^q_{\sigma_k} = C^\delta_{\sigma_k}, \qquad D^q_{\sigma_k} = D^\delta_{\sigma_k} \tag{15}$$

$$Q^q_{\sigma_k} = \Delta Q^\delta_{\sigma_k}, \qquad R^q_{\sigma_k} = \Delta^{-1} R^\delta_{\sigma_k}, \qquad S^q_{\sigma_k} = S^\delta_{\sigma_k}. \tag{16}$$

# 3 Maximum Likelihood estimation and the EM algorithm

To estimate the parameters, we use the Maximum likelihood (ML) estimator defined as

$$\hat{\beta} = \arg\max_{\beta} \ell(\beta), \tag{17}$$

where the log-likelihood function $\ell(\beta)$ is given by

$$\ell(\beta) = \log p(Y_N|\beta), \tag{18}$$

and where $\beta = [\theta^T \ [\vec{Q}^c]^{-T} \ [\vec{R}^c]^{-T}]^T$. The operator $\vec{X}$ creates a vector from a matrix $X$ by stacking it columns on one another. $p(Y_N|\beta)$ denotes the probability distribution of $Y_N := \{y_1, y_2, \ldots, y_N\}$ given the parameter $\beta$. We call $Y_N$ the measurements. For future reference, we also define $X_N := \{x_1, x_2, \ldots, x_N\}$. The maximization of the log-likelihood function defined in (18), for state space models, is a non-convex problem [12]. In this context, it is helpful to use iterative algorithms such as Newton-Raphson or the Expectation Maximization (EM) algorithm [22] to facilitate the computations. The EM algorithm is known to converge to a stationary point of the likelihood function. However, local minima may be also a problem and thus the initialization of the estimates is an important issue.

**Assumption 1** *The vector of parameters* $\beta$, *the input* $(u_k)$ *and the noise* $(w_k)$ *satisfy regularity conditions guaranteeing that the solution* $\hat{\beta}$ *of the optimization problem in* (17) *converges (in probability or a.s.) to the true solution* $\beta_0$.

Assumption (1) is necessary, for example, to assure system identifiability. For example, if the collection of switching systems never considers one component of the parameter vector $\beta$, then we cannot identify the missing parameter. In particular, if the conditions of theorem 3.6 in [23, p.31] are satisfied, then $\lim_{N\to\infty} \hat{\beta} = \beta_0$ (in probability or a.s.). Such conditions are very general, and it is necessary to specialize them for every particular problem.

The EM algorithm is an iterative method that generates a sequence of estimates $\hat{\beta}^{(i)}$, $i = 1, 2, \ldots$, of the parameter vector $\beta$. These estimates converge to a local maximum of the log-likelihood function. The EM algorithm consists of two steps: (i) an expectation step (E-step), and (ii) a maximization step (M-step). The EM algorithm can be summarised as follows:

(i) Start with an initial estimate of the system parameter $\beta_o$,

(ii) E-step: Obtain the function $\mathcal{Q}(\beta, \hat{\beta}^{(i)})$, which corresponds to the expected value of the log-likelihood for the complete data $(X_N, Y_N)$ given the observed data $Y_N$,

(iii) M-step: Maximize the function $\mathcal{Q}(\beta, \hat{\beta}^{(i)})$ with respect to the parameter $\theta$. This yields a new parameter estimate,

$$\hat{\beta}^{(i+1)} = \arg\max_{\beta} \mathcal{Q}(\beta, \hat{\beta}^{(i)}). \tag{19}$$

(iv) Set $i \to i+1$, and return to (ii) until convergence.

### 3.1 Calculation of $\mathcal{Q}$ for discrete-time systems

We note that the system switches between different sub-systems. At sampling time $k$, $\sigma_k \in \{1, \ldots, m\}$. Considering this, we have the following:

**Lemma 2** *For the system described in* (14)*, with* $\sigma_k \in \{1, \ldots, m\}$*, the auxiliary function* $\mathcal{Q}$ *of the EM algorithm is given by*

$$\begin{aligned}\mathcal{Q} = &-\frac{1}{2}\log\det\{P_0\} - \frac{N}{2}\log\det\{P\} - \frac{1}{2}tr\{P_0^{-1}[(\hat{x}_{0|Y_N} - \mu_0)(\hat{x}_{0|Y_N} - \mu_0)^T + \Sigma_{0|Y_N}]\} \\ &- \frac{1}{2}\sum_{j=1}^{m} tr\{P^{-1}[\Xi_j - \psi_j\Theta_j^T - \Theta_j\psi_j^T + \Theta_j\phi_j\Theta_j^T]\}\end{aligned} \tag{20}$$

*where*

$$\Theta_j = \begin{bmatrix} A_{\sigma_k} & B_{\sigma_k} \\ C_{\sigma_k} & D_{\sigma_k} \end{bmatrix}_{\sigma_k = j}, \quad \xi_k = \begin{bmatrix} x_{k+1} \\ y_k \end{bmatrix}, \quad z_k = \begin{bmatrix} x_k \\ u_k \end{bmatrix}, \quad P = \begin{bmatrix} Q^q & S^q \\ [S^q]^T & R^q \end{bmatrix} \tag{21}$$

$$\Xi_j = \sum_{k:\sigma_k=j} \Sigma_{\xi_k}, \quad \psi_j = \sum_{k:\sigma_k=j} \Sigma_{\xi_k z_k}, \quad \phi_j = \sum_{k:\sigma_k=j} \Sigma_{z_k z_k}, \tag{22}$$

*and*

$$\hat{x}_{0|Y_N} = \mathbb{E}\{x_0|Y_N, \hat{\beta}^{(i)}\} \tag{23}$$

$$\hat{\xi}_k = \mathbb{E}\{\xi_k|Y_N, \hat{\beta}^{(i)}\} \tag{24}$$

$$\hat{z}_k = \mathbb{E}\{z_k|Y_N, \hat{\beta}^{(i)}\} \tag{25}$$

$$\Sigma_{0|Y_N} = \mathbb{E}\{(x_0 - \hat{x}_{0|Y_N})(x_0 - \hat{x}_{0|Y_N})^T|Y_N, \hat{\beta}^{(i)}\} \tag{26}$$

$$\Sigma_{\xi_k} = \mathbb{E}\{(\xi_k - \hat{\xi}_k)(\xi_k - \hat{\xi}_k)^T|Y_N, \hat{\beta}^{(i)}\} \tag{27}$$

$$\Sigma_{\xi_k z_k} = \mathbb{E}\{(\xi_k - \hat{\xi}_k)(z_k - \hat{z}_k)^T|Y_N, \hat{\beta}^{(i)}\} \tag{28}$$

$$\Sigma_{z_k} = \mathbb{E}\{(z_k - \hat{z}_k)(z_k - \hat{z}_k)^T|Y_N, \hat{\beta}^{(i)}\} \tag{29}$$

**Proof** Since the resulting process is Gaussian, we can follow a similar procedure to that in [24]. If we have only one system to estimate (i.e., $\Theta$ is common for each sub-system) then, the expression for $\mathcal{Q}$ in (20) is the same as the one given in [24]. However, in our problem, we have different sub-systems. Thus, the expressions in (22) have to be calculated for each $\Theta_j$. These, in turn, depend on the switching sequence $\sigma_k$. ■

**Remark 3** *The optimization of the auxiliary function* $\mathcal{Q}$ *in* (20) *is rather complex since the covariances* $Q^q_{\sigma_k}$*, and* $R^q_{\sigma_k}$ *depend on the sequence signal* $\sigma_k$*. In addition, there is an extra term,* $S^q_{\sigma_k}$*, that needs to be considered.*

**Remark 4** *When the discrete-time system is expressed in incremental (or* delta*) form, it closely resembles the continuous-time representation in* (1)*. In fact, as the sampling time* $\Delta \to 0$*, then the incremental form representation approaches the continuous-time representation. Thus, we have*

$$A^{\delta}_{\sigma_k} \to A^{c}_{\sigma_k}, \qquad B^{\delta}_{\sigma_k} \to B^{c}_{\sigma_k}, \tag{30}$$

$$C^{\delta}_{\sigma_k} \to C^{c}_{\sigma_k}, \qquad D^{\delta}_{\sigma_k} \to D^{c}_{\sigma_k}, \tag{31}$$

$$\begin{bmatrix} Q^{\delta} & S^{\delta} \\ [S^{\delta}]^T & R^{\delta} \end{bmatrix} \to \begin{bmatrix} Q^{c} & 0 \\ 0 & R^{c} \end{bmatrix}. \tag{32}$$

### 3.2 Calculation of $\mathcal{Q}$ for *delta* form systems

Next we show that the auxiliary function $\mathcal{Q}$ can be expressed in a more convenient form for the system in (8). We have the following:

**Lemma 3** *When* $\Delta \to 0$*, the E-step given in* (20) *can be written as*

$$\begin{aligned} \mathcal{Q} = &-\frac{1}{2} tr\{[Q^{\delta}]^{-1}[\mathbf{\Phi I} - (\mathbf{\Psi} - \mathbf{\Upsilon})[\mathbf{A}^{\delta}, \mathbf{B}^{\delta}]^T - [\mathbf{A}^{\delta}, \mathbf{B}^{\delta}](\mathbf{\Psi} - \mathbf{\Upsilon})^T + [\mathbf{A}^{\delta}, \mathbf{B}^{\delta}]\mathbf{\Gamma}[\mathbf{A}^{\delta}, \mathbf{B}^{\delta}]^T]\} \\ &- -\frac{1}{2} tr\{[R^{\delta}]^{-1}[\mathbf{\Omega I} - \mathbf{\Lambda}[\mathbf{C}^{\delta}, \mathbf{D}^{\delta}]^T - [\mathbf{C}^{\delta}, \mathbf{D}^{\delta}]\mathbf{\Lambda}^T + [\mathbf{C}^{\delta}, \mathbf{D}^{\delta}]\mathbf{\Pi}[\mathbf{C}^{\delta}, \mathbf{D}^{\delta}]^T]\} \end{aligned} \tag{33}$$

*where*

$$\mathbf{\Phi} = \begin{bmatrix} \Phi_1 & \dots & \Phi_m \end{bmatrix}, \quad \mathbf{\Psi} = \begin{bmatrix} \Psi_1 & \dots & \Psi_m \end{bmatrix}, \tag{34}$$

$$\mathbf{\Upsilon} = \begin{bmatrix} \Upsilon_1 & \dots & \Upsilon_m \end{bmatrix}, \tag{35}$$

$$\mathbf{\Omega} = \begin{bmatrix} \Omega_1 & \dots & \Omega_m \end{bmatrix}, \quad \mathbf{\Lambda} = \begin{bmatrix} \Lambda_1 & \dots & \Lambda_m \end{bmatrix}, \tag{36}$$

$$\mathbf{\Gamma} = \begin{bmatrix} \Gamma_1 & 0 & \dots \\ 0 & \ddots & 0 \\ \vdots & 0 & \Gamma_m \end{bmatrix}, \quad \mathbf{\Pi} = \begin{bmatrix} \Pi_1 & 0 & \dots \\ 0 & \ddots & 0 \\ \vdots & 0 & \Pi_m \end{bmatrix}, \quad \mathbf{I} = \begin{bmatrix} I \\ \vdots \\ I \end{bmatrix}, \tag{37}$$

*and*

$$\Phi_j = \sum_{k:\sigma_k = j} \Delta^{-1} \mathbb{E}\{(x_k - x_{k-1})(x_k - x_{k-1})^T | Y_N, \hat{\beta}^{(i)}\} \tag{38}$$

$$\Psi_j = \sum_{k:\sigma_k = j} \mathbb{E}\{x_k z_{k-1}^T | Y_N, \hat{\beta}^{(i)}\} \tag{39}$$

$$\Upsilon_j = \sum_{k:\sigma_k = j} \mathbb{E}\{x_{k-1} z_{k-1}^T | Y_N, \hat{\beta}^{(i)}\} \tag{40}$$

$$\Gamma_j = \sum_{k:\sigma_k = j} \Delta \mathbb{E}\{z_{k-1} z_{k-1}^T | Y_N, \hat{\beta}^{(i)}\} \tag{41}$$

$$\Omega_j = \sum_{k:\sigma_k = j} \Delta y_k y_k^T \tag{42}$$

$$\Lambda_j = \sum_{k:\sigma_k = j} \mathbb{E}\{y_k z_k^T | Y_N, \hat{\beta}^{(i)}\} \tag{43}$$

$$\Pi_j = \sum_{k:\sigma_k = j} \mathbb{E}\{z_k z_k^T | Y_N, \hat{\beta}^{(i)}\}. \tag{44}$$

**Proof** We follow a similar procedure as in [12]. We begin by substituting $P = \begin{bmatrix} \Delta Q^\delta & 0 \\ 0 & \Delta^{-1} R^\delta \end{bmatrix}$ into (20). Developing the expressions, we obtain:

$$\begin{aligned} \mathcal{Q} = &-\frac{1}{2}\sum_j \mathrm{tr}\{(Q^\delta)^{-1}\Big[\Phi_j - (\Psi_j - \Upsilon_j)[A^\delta, B^\delta]^T - [A^\delta, B^\delta](\Psi_j - \Upsilon_j)^T + [A^\delta, B^\delta]\Gamma_j[A^\delta, B^\delta]^T\Big]\} \\ &-\frac{1}{2}\sum_j \mathrm{tr}\{(R^\delta)^{-1}\Big[\Omega_j - \Lambda_j[C^\delta, D^\delta]^T - [C^\delta, D^\delta]\Lambda_j^T + [C^\delta, D^\delta]\Pi_j[C^\delta, D^\delta]^T\Big]\}. \end{aligned} \tag{45}$$

Writing (45) using matrices, we obtain (33). ■

**Lemma 4** *The function $\mathcal{Q}$ in* (33) *can be written as:*

$$\begin{aligned} \mathcal{Q} = &-\frac{1}{2}\Big[\alpha_1^T[\mathbf{\Gamma} \otimes [Q^\delta]^{-1}]\alpha_1 - 2(\mathbf{\Psi} - \mathbf{\Upsilon})^T[I \otimes [Q^\delta]^{-1}]\alpha_1 + tr\{[Q^\delta]^{-1}\mathbf{\Phi}\}\Big] \\ &-\frac{1}{2}\Big[\alpha_2^T[\mathbf{\Pi} \otimes [R^\delta]^{-1}]\alpha_2 - 2\mathbf{\Lambda}^T[I \otimes [R^\delta]^{-1}]\alpha_2 + tr\{[R^\delta]^{-1}\mathbf{\Omega}\}\Big] \end{aligned} \tag{46}$$

*where* $\alpha_1 = \begin{bmatrix} \vec{\mathbf{A}}^\delta \\ \vec{\mathbf{B}}^\delta \end{bmatrix}$, *and* $\alpha_2 = \begin{bmatrix} \vec{\mathbf{C}}^\delta \\ \vec{\mathbf{D}}^\delta \end{bmatrix}$, *with*

$$\begin{bmatrix} \vec{\mathbf{A}}^\delta \\ \vec{\mathbf{B}}^\delta \end{bmatrix} = \begin{bmatrix} \vec{A}_1^\delta \\ \vec{B}_1^\delta \\ \vdots \\ \vec{A}_m^\delta \\ \vec{B}_m^\delta \end{bmatrix}, \quad \begin{bmatrix} \vec{\mathbf{C}}^\delta \\ \vec{\mathbf{D}}^\delta \end{bmatrix} = \begin{bmatrix} \vec{C}_1^\delta \\ \vec{D}_1^\delta \\ \vdots \\ \vec{C}_m^\delta \\ \vec{D}_m^\delta \end{bmatrix}, \tag{47}$$

*and*

$$\alpha_1 = \mathbf{L}^1\theta + \mathbf{b}^1, \quad \alpha_2 = \mathbf{L}^2\theta + \mathbf{b}^2, \tag{48}$$

*with*

$$\mathbf{L}^1 = \begin{bmatrix} [L_1^1]^T & \dots & [L_m^1]^T \end{bmatrix}^T, \quad \mathbf{b}^1 = \begin{bmatrix} [b_1^1]^T & \dots & [b_m^1]^T \end{bmatrix}^T \tag{49}$$

$$\mathbf{L}^2 = \begin{bmatrix} [L_1^2]^T & \dots & [L_m^2]^T \end{bmatrix}^T, \quad \mathbf{b}^2 = \begin{bmatrix} [b_1^2]^T & \dots & [b_m^2]^T \end{bmatrix}^T. \tag{50}$$

**Proof** We use standard properties of *trace*, *vec* and *Kronecker* operators. In addition, since each of the matrices $(A_{\sigma_k}^\delta, B_{\sigma_k}^\delta, C_{\sigma_k}^\delta, D_{\sigma_k}^\delta)$ is a function of $\theta$, then we can write $\alpha_1$ and $\alpha_2$ as in (48).

### 3.3 The M-step

The M-step in the EM algorithm corresponds to the optimization of the auxiliary function $\mathcal{Q}$ in (46). Unfortunately, this step does not have a closed form. To tackle this problem, we utilize the idea inherent in generalized EM (GEM) type algorithms, where one seeks to increase the value of the function $\mathcal{Q}$ at each maximization step [25, 26, 27] (i.e., $\mathcal{Q}(\hat{\beta}^{i+1}, \hat{\beta}^i) > \mathcal{Q}(\hat{\beta}^i, \hat{\beta}^i)$), rather than maximizing it. In particular, we use the, so-called, expectation conditional maximization (ECM) algorithm. When applied to our problem, the ECM algorithm consists of alternatively maximizing

the function $\mathcal{Q}$ with respect to $\theta$ first, and then with respect to $[Q^\delta]^{-1}$ $[R^\delta]^{-1}$. The ECM algorithm ensures that the log-likelihood function monotonically increases at each iteration [28, p.394]. We then have:

**Theorem 1** *The M-step for the problem of interest is given by:*

*(i) For frozen $Q^\delta$ and $R^\delta$:*

$$\theta = \Big([\mathbf{L}^1]^T[\mathbf{\Gamma}\otimes[Q^\delta]^{-1}]\mathbf{L}^1 + [\mathbf{L}^2]^T[\mathbf{\Pi}\otimes[R^\delta]^{-1}]\mathbf{L}^2\Big)^{-1}\Big([\mathbf{L}^1]^T([I\otimes[Q^\delta]^{-1}]^T(\mathbf{\Psi}-\mathbf{\Upsilon}) - [\mathbf{\Gamma}\otimes[Q^\delta]^{-1}]\mathbf{b}^1) + [\mathbf{L}^2]^T([I\otimes[R^\delta]^{-1}]^T\mathbf{\Lambda} - [\mathbf{\Pi}\otimes[R^\delta]^{-1}]\mathbf{b}^2)\Big) \tag{51}$$

*(ii) For frozen $A^\delta$,$B^\delta$,$C^\delta$,$D^\delta$:*

$$Q^\delta = \frac{1}{N}\Big(\mathbf{\Phi I} - (\mathbf{\Psi}-\mathbf{\Upsilon})[\mathbf{A}^\delta,\mathbf{B}^\delta]^T - [\mathbf{A}^\delta,\mathbf{B}^\delta](\mathbf{\Psi}-\mathbf{\Upsilon})^T + [\mathbf{A}^\delta,\mathbf{B}^\delta]\mathbf{\Gamma}[\mathbf{A}^\delta,\mathbf{B}^\delta]^T\Big), \tag{52}$$

$$R^\delta = \frac{1}{N}\Big(\mathbf{\Omega I} - \mathbf{\Lambda}[\mathbf{C}^\delta,\mathbf{D}^\delta]^T - [\mathbf{C}^\delta,\mathbf{D}^\delta]\mathbf{\Lambda}^T + [\mathbf{C}^\delta,\mathbf{D}^\delta]\mathbf{\Pi}[\mathbf{C}^\delta,\mathbf{D}^\delta]^T\Big). \tag{53}$$

**Proof** We substitute (48) into (46), and then differentiate the resulting expression with respect to $\theta$. We obtain:

$$\begin{aligned}-2\frac{\partial\mathcal{Q}}{\partial\theta} = {}& 2[\mathbf{L}^1]^T[\mathbf{\Gamma}\otimes Q^{-1}](\mathbf{L}^1\theta+\mathbf{b}^1) - 2[\mathbf{L}^1]^T[I\otimes Q^{-1}]^T(\mathbf{\Psi}-\mathbf{\Upsilon}) + \\ & 2[\mathbf{L}^2]^T[\mathbf{\Pi}\otimes R^{-1}](\mathbf{L}^2\theta+\mathbf{b}^2) - 2[\mathbf{L}^2]^T[I\otimes R^{-1}]^T(\mathbf{\Psi}-\mathbf{\Lambda})\end{aligned} \tag{54}$$

If we set (54) equal to zero and solve for $\theta$, we obtain the expression in (51). Similarly, if we differentiate (46) with respect to $[Q^\delta]$ and $[R^\delta]$, we obtain (52) and (53), respectively. ■

Finally, we can bring all of the elements together:

## Algorithm to estimate continuous-time switching systems

(i) Start with an initial estimate for $\beta$, namely $\hat{\beta}^{(i)}$, and a known switching sequence $\sigma_k$, $k = 1,\ldots,N$,

(ii) Calculate the sets defined in (3) and (4),

(iii) Calculate expressions (38) to (44), followed by expressions (34) to (37),

(iv) Calculate the constraints in (48),

(v) For frozen $[Q^\delta]^{(i)}$ and $[R^\delta]^{(i)}$, calculate a *new* value for the parameter $\theta$, namely $\hat{\theta}^{(i+1)}$ from (51),

(vi) With the new value of $\theta$ obtained in (v), $\hat{\theta}^{(i+1)}$, re-calculate (ii) and (iii) and, from (52) and (53), obtain new values for $Q^\delta$, and $R^\delta$, namely $[Q^\delta]^{(i+1)}$, and $[R^\delta]^{(i+1)}$, respectively,

(vii) Set $i \to i+1$, and return to (i) until convergence.

# 4 Identification in power electronics

Here we investigate the application of the general tools developed above to specific problems in power electronics.

## 4.1 Background

In power electronics, four particular identification problems can be distinguished based on practical requirements (see Fig. 1):

(i) *Internal Identification:* Due to the switching nature of the devices, internal power converter components are, in general, exposed to high electrical stress, such as high-blocking-voltage, pulsating currents, and high temperature, see e.g. [29]. This may result in performance degradation of the converter over time, or even, in some cases internal faults [30]. In particular, the large amount of passive and active components utilized in multilevel converters increases the probability of faults, reducing the reliability of these switched systems [30, 31] . Even though several fault detection and fault tolerant strategies for power converters have been proposed (see e.g. [32, 33, 34, 31]), performance following a fault is, in general, poor [31]. For this reason, it is often desirable to implement some form of health monitoring system to evaluate the state of health of the power converter by identifying the internal components in order to avoid faults [35] .

(ii) *External Identification:* Power converters are intended to electrically feed different kinds of load with different parameter values. For this reason, one will often be interested in identifying the load parameters so that one can adjust the converter settings in order to satisfy the load requirements. This is especially important in the case of electrical machine control [36, 21, 37]. Additionally, load parameter identification can be also used to carry out fault analysis of the electrical load [38].

(iii) *Entire System Identification:* Usually, when carrying out identification of load parameters, it is assumed that the power converter is an ideal power source, neglecting its internal dynamics, see e.g. [39]. This identification procedure, in general, improves the performance of the underlying estimation process needed to implement control feedback strategies. However, this approximation may lead to errors in the identification process, especially in the case of multilevel converters where more internal passive and active components are involved in the full system (i.e. converter+load) dynamics [6].

(iv) *Unknown Switching States:* It is common (and we will adopt this premise) to assume that the switching sequence is known. However, the switching sequence can be affected by power switching faults or mistrigger pulses [34]. For this reason, one may also be interested in identifying the switching sequence itself. The interested reader is referred to [1, 11] for identification of the switching sequence based on stochastic approaches.

In the current paper, we will focus on the first case, i.e., the *internal identification* problem. The challenge here comes from the fact that power converters are hybrid or switched (non)linear systems [3]. These kind of systems can be described by a set of discrete modes (where each mode in the

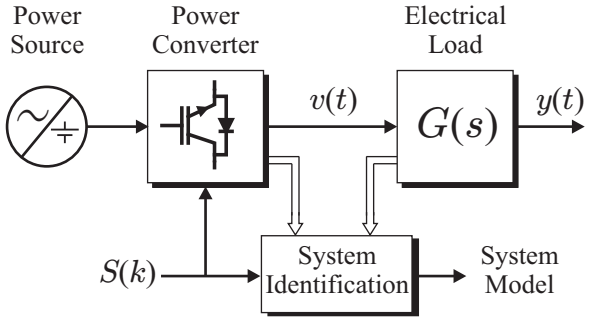


Figure 1: System identification process for power converters.

set corresponds to a different state of the power switches) with an associated continuous dynamic model (involving voltages, currents, etc.). Switches trigger events that lead to jumps between the different modes.

### 4.2 Illustrative Case: Application to multicell converter

As an illustrative example, we propose to analyze the internal identification problem for a particular class of power converters called Flying Capacitor Converters (FCC). This class of multilevel converter has attracted significant attention due to the fact that this topology requires only one main DC-voltage to electrically feed the entire system [40]. As depicted in Fig. 2, FCCs comprise multiple interconnected cells. Each cell contains a pair of complementary switches, $S_i$ and $\overline{S}_i$, and a capacitor, $C_i$. These are used to synthesize intermediate output voltage levels [21, 40, 41, 42, 43]. Due to its configuration, this converter is also known as a *multicell converter*. To increase the reliability of the floating capacitors, self-healing capacitors can be used [32]. Nevertheless, these electrical components experience capacitance degradation due to the effect of current harmonics and internal faults [44]. Thus, we propose an identification methodology which allows one to estimate the actual capacitance value of the internal floating capacitors, $C_i$. This information can then be used to evaluate the health of the power converter.

For our problem, the system state and system output are represented by $x = [v_{c1} \quad v_{c2} \quad i_a]^T$ and $y = i_a$ respectively, while $s = [s_1 \quad s_2 \quad s_3]^T$ stands for the switching elements, which can only take two values, $s_i = 0$ if the switch is open and $s_i = 1$ if it is closed, i.e., $s_i \in \{0, 1\}$, for all $i \in \{1, 2, 3\}$. Consequently, the switching elements are restricted to belong to the following finite set:

$$\mathbb{S} = \left\{ \begin{bmatrix} 0 \\ 0 \\ 0 \end{bmatrix}, \begin{bmatrix} 1 \\ 0 \\ 0 \end{bmatrix}, \begin{bmatrix} 0 \\ 1 \\ 0 \end{bmatrix}, \begin{bmatrix} 1 \\ 1 \\ 0 \end{bmatrix}, \begin{bmatrix} 0 \\ 0 \\ 1 \end{bmatrix}, \begin{bmatrix} 1 \\ 0 \\ 1 \end{bmatrix}, \begin{bmatrix} 0 \\ 1 \\ 1 \end{bmatrix}, \begin{bmatrix} 1 \\ 1 \\ 1 \end{bmatrix} \right\}. \tag{55}$$

The disturbance-free continuous-time dynamic model of the system, when feeding an $rl$-electrical load, can be represented as:

$$\begin{aligned} \frac{dx(t)}{dt} &= A^c(s(t))x(t) + B^c(s(t)), \\ y(t) &= C^c x(t), \end{aligned} \tag{56}$$

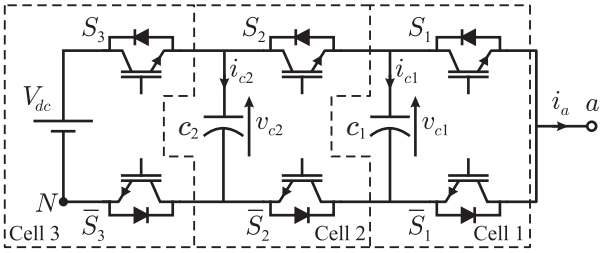


Figure 2: Three-cell flying capacitor converter.

where

$$A^c(s(t)) = \begin{bmatrix} 0 & 0 & \frac{s_2(t)-s_1(t)}{c_1} \\ 0 & 0 & \frac{s_3(t)-s_2(t)}{c_2} \\ \frac{s_1(t)-s_2(t)}{l} & \frac{s_2(t)-s_3(t)}{l} & -\frac{r}{l} \end{bmatrix},$$
$$B^c(s(t)) = \begin{bmatrix} 0 \\ 0 \\ s_3(t)\frac{V_{dc}}{l} \end{bmatrix}, \quad C^c = [0 \quad 0 \quad 1]^T. \tag{57}$$

In this model, parameters $r, l, c_1$, and $c_2$ are the load resistance, load inductance, and the 2 internal capacitance values, respectively.

Since $s(t) \in \mathbb{S}$, the FCC model presented in (56) is a special case (where $u(t)$ is constant) of the hybrid model described in (1), where $\sigma(t) \in \{1, \ldots, 8\}$ stands for the different system modes triggered by the switching elements, $s(t) \in \mathbb{S}$. Thus, the pair $(A^c_{\sigma(t)}, B^c_{\sigma(t)}) \in \{(A^c_1, B^c_1), \ldots, (A^c_8, B^c_8)\}$.

We are interested in obtaining an estimate of the following FCC parameters

$$\theta = \{c_1, c_2\}. \tag{58}$$

These parameters are present in the different subsystems through the matrix $A^c_{\sigma(t)}(\theta)$. Next, we describe results based on simulation and experimental work carried out in our laboratory.

**Remark 5** *Note that the voltages in the capacitors $v_{c1}$ and $v_{c2}$ remain constant when $s_1(t) = s_2(t)$ and $s_2(t) = s_3(t)$, respectively. This, in turn, implies that the sums in* (38)-(44) *should consider a reduced number of terms.*

### 4.2.1 Simulation Results

As described in Section 4, in our particular problem we have $m = 8$ different subsystems with the following common parameters: $V_{dc} = 150\ V$, $r = 30\ \Omega$, $l = 10\ mH$, and "true" (nominal) values of $c_1 = c_2 = 110\ \mu F$.

The spectral densities of the continuous-time process and measurement noise are chosen as

$$Q^c = 10^3 \begin{bmatrix} 1 & 0 & 0 \\ 0 & 1 & 0 \\ 0 & 0 & 0.0001 \end{bmatrix}, \quad R^c = 5 \times 10^{-7}.$$

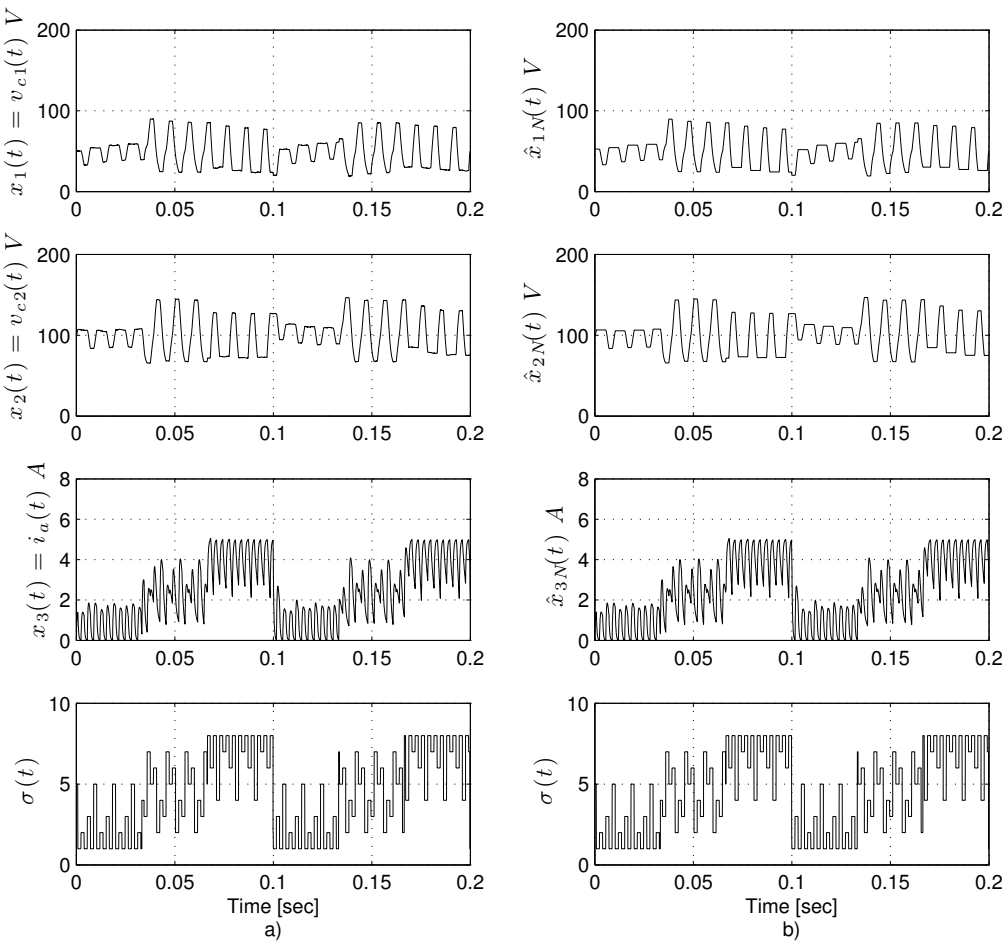


Figure 3: Simulation Results: Continuous-time system state dynamics: a) actual system state $x(t)$ and the system input $\sigma(t)$; b) system state estimate $\hat{x}(k)$ after completion of the identification algorithm.

To implement the EM algorithm we consider a data length of N=4000, which is obtained with a sampling frequency of $f_s = 20kHz$, i.e., $\Delta = 50\mu s$. This is a standard sampling frequency used to control this converter; see e.g., [42]. This sampling period is sufficiently faster than the dynamics of the capacitor voltages given by $\tau_c = r \times c \approx 3.3\ m$, resulting in $\Delta = 66\tau_c$. Consequently, the EM identification algorithm can be carried out considering the sampled-data model as presented in Section 3 assuming that $A^{\delta}_{\sigma_k}(\theta) = A^{c}_{\sigma_k}(\theta)$, $B^{\delta}_{\sigma_k} = B^{c}_{\sigma_k}$, $C^{\delta}_{\sigma_k} = C^{c}$, $D^{\delta}_{\sigma_k} = 0$, $Q^{\delta}_{\sigma_k} = Q^{c}$, $R^{\delta}_{\sigma_k} = R^{c}$, and $S^{\delta}_{\sigma_k} = 0_{1\times 3}$.

The switching sequence is chosen in order to emulate standard Phase-Shifted Pulse-Width Modulation (PS-PWM). Here, each pair of switches is commuted with an identical switching sequence with a period of $h = 192\Delta$ and a phase shift between consecutive cells of $h/3$. PS-PWM guarantees that, in open loop, the floating voltages $v_{c1}$ and $v_{c2}$ will oscillate around the values $V_{dc}/3$ and $2V_{dc}/3$ respectively [40]. To initialize the algorithm, we consider $Q^{c}_{0} = 0.5Q^{c}$, $R^{c}_{0} = 1.5R^{c}$, and

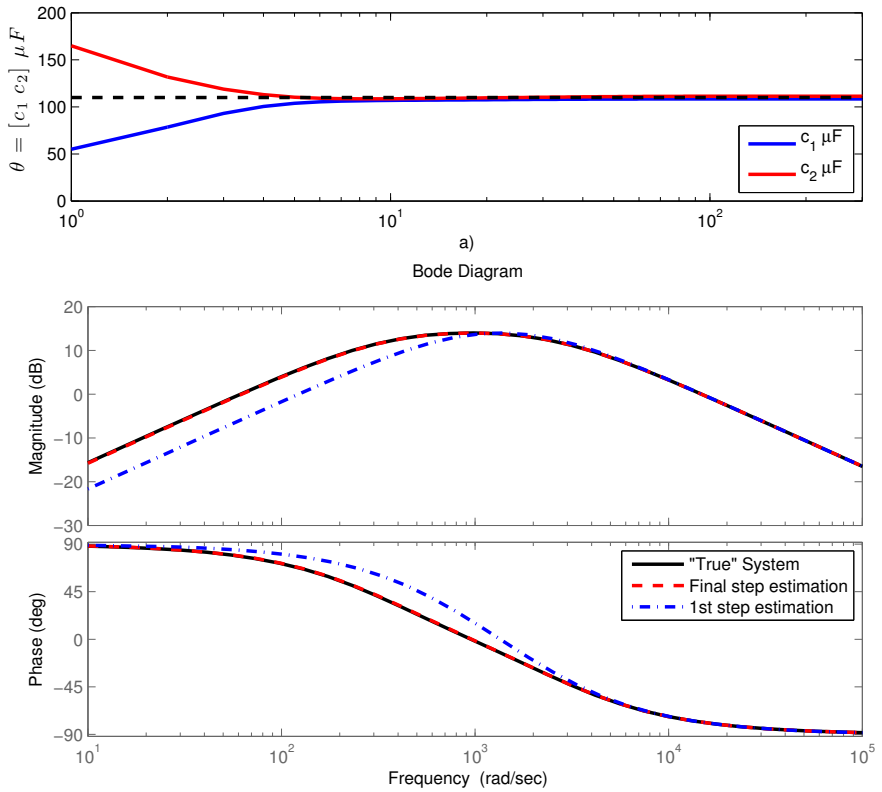


Figure 4: Simulation Results: System identification results.

$\theta_0 = [1.5c_1\ 0.5c_2]$.

The data window used to estimate the internal capacitance is shown in Fig. 3. The actual system state, $x(t)$, is depicted in Fig. 3-a) while the system estimate, $\hat{x}(t)$ is presented in Fig. 3-b). In both cases the same switching sequence, $\sigma(t)$, is considered. It can be observed that the state estimates closely resemble the actual system state.

The simulation result of the estimation is shown in Fig, 4-a). Here, one can see that the estimated parameters achieve the "true" (nominal) capacitance values after 100 iterations of the EM algorithm. To verify the performance of the proposed algorithm in terms of system identification, Fig. 4-b) shows the Bode diagram of the system (input: $V_{dc}$, output: $i_a$), with $\sigma = 5$ (black line), along with the first step estimation (dot-dashed blue line), and the final step estimation (dashed red line). Clearly, the final system frequency response is the same as the continuous-time dynamics of the "true" system.

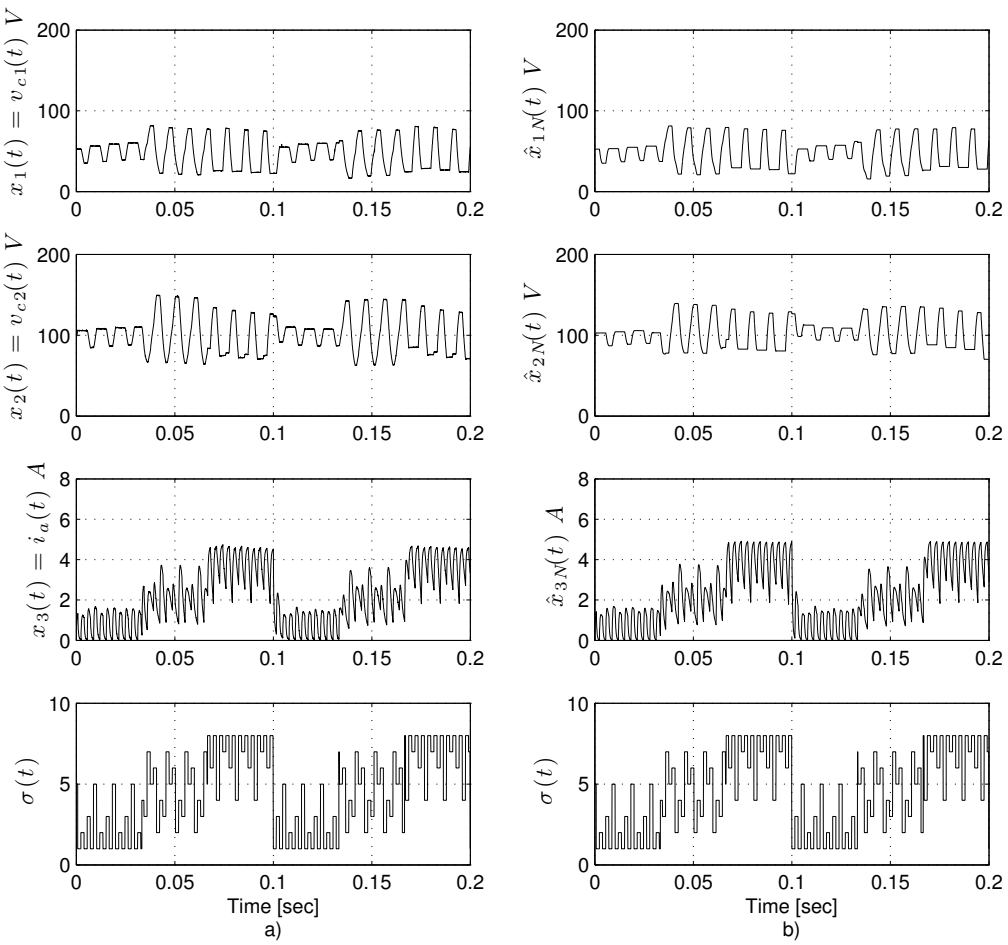


Figure 5: Experimental Results: Continuous-time system state dynamics: a) measured system state $x(t)$ and the system input $\sigma(t)$; b) system state estimate $\hat{x}(k)$ after completion of the identification algorithm.

### 4.2.2 Experimental Results

To verify the performance of the proposed identification algorithm, experiment studies were carried out in our laboratory. The experiments were performed on an FCC laboratory prototype. This converter was built based on discrete insulated-gate bipolar transistors (IGBTs) IRG4PC30KD and standard electrolytic capacitors with a nominal capacitance of $c_1 = c_2 = 110\mu F$. It is important to emphasize that the nominal capacitance presents a tolerance of $\pm 20\%$. The remaining nominal electrical parameters of the converter-load system are chosen to be the same as in the simulation study, i.e., $V_{dc} = 150\ V$, $r = 30\ \Omega$ and $L = 10\ mH$. To capture the data a digital platform based on a TMS320C6713 DSP along with an XC3S400 FPGA was used. This is a standard digital platform used to handle power converters; see e.g., [34, 42, 45]. Thus, similar to the simulation case, we obtained a length of measured data of $N = 4000$ sampled at $f_s = 20kHz$. To initialize the algorithm, we consider the same initial value for the covariance as in the simulation case.

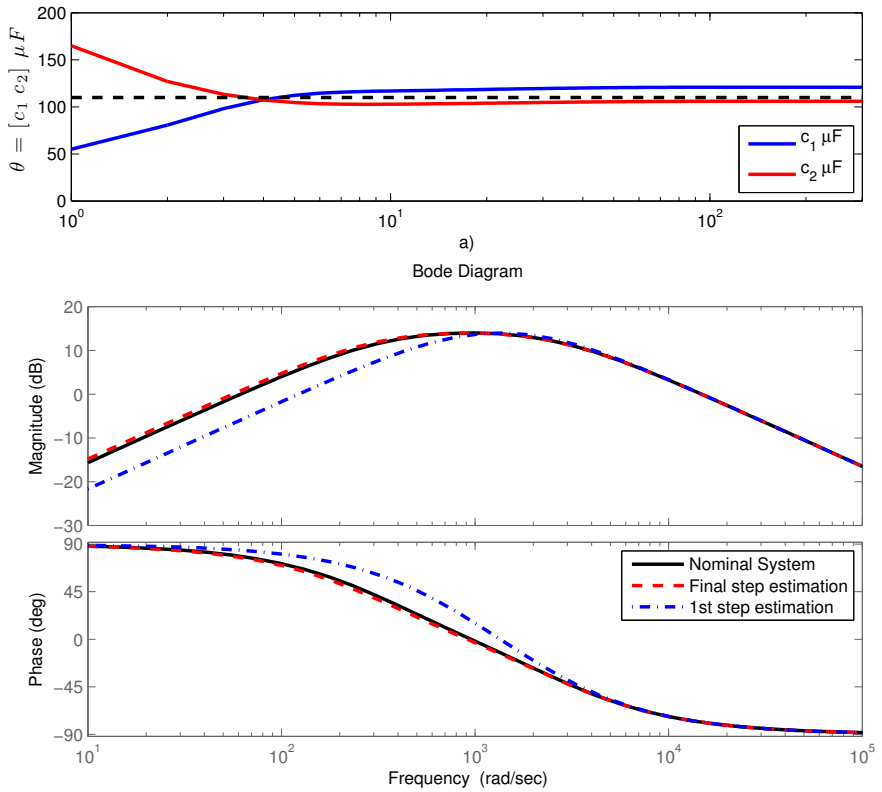


Figure 6: Experimental Results: System identification results.

The experimental data window used to estimate the internal capacitance is shown in Fig. 5. Since the "true" system is unknown, the measured system state, $x(t)$, is presented in Fig. 5-a) while the system estimate, $\hat{x}(t)$ is presented in Fig. 3-b). Notice that, in this case, we consider the same switching sequence, $\sigma(t)$, than in the simulation case. This allows one to compare the experimental to the simulation results. Here, one can clearly observe that the system model (56)-(57) closely describes the actual FCC continuous-time dynamics.

The experimental result of the proposed estimation algorithm is presented in Fig. 6. Here, one can see that the estimated parameters achieve a value close to the nominal one after 100 iterations of the EM algorithm (similar to the simulation case), i.e., $c_1 = 121\mu F$ and $c_2 = 106\mu F$. Notice that these values are within the corresponding tolerance (error) for this kind of capacitors.

In Fig. (6)-b), the Bode diagram of the system (input: $V_{dc}$, output: $i_a$), with $\sigma = 5$ (black line), along with the first step estimation (blue line) and the final step estimation (red line) is presented. The bode diagram confirms that, even when there exist a small error between the nominal and estimated parameters, the final system frequency response closely resembles the nominal continuous-time system dynamics.

# 5 Conclusions

In this work, we have proposed an EM based identification algorithm for switched linear systems. The key idea of our proposal comes from the fact that a change in system modes can only be triggered at the sampling instants. Additionally, we have shown that, by considering fast-sampling, one can use the incremental-form model to directly estimate the continuous-time system model parameters, allowing one to reduce the EM algorithm complexity, as shown in Section 3.

As an illustrative example, we have implemented this algorithm to estimate the internal capacitor values of a multicell converter. The proposed methodology can be used to monitor the health condition of the floating capacitors. Both simulation and experimental results show that the formulation of the EM algorithm in terms of incremental-form models provides good numerical behaviour for fast-sampling rates. Thus, one can conclude that the proposed approach provides a direct way to estimate continuous-time switched linear systems.

Future work will be focused on switching sequence design for hybrid systems. This is an interesting problem. There are associated difficulties arising from the fact that all reachable modes have to be sufficiently excited in order to improve the estimation of system parameters. Additionally, it is important to investigate how to implement this identification algorithm in closed-loop, in order to achieve both, control and identification of power converters.

# References


[1] J. D. Hamilton, "Analysis of time series subject to changes in regime," *Journal of econometrics*, vol. 45, no. 1, pp. 39–70, 1990.

[2] A. J. van der Schaft and J. M. Schumacher, "An introduction to hybrid dynamical systems," Springer, 2000.

[3] M. Senesky and G. Eirea, "Hybrid modelling and control of power electronics," in *Hybrid Systems: Computation and Control*, O. Maler and A. Pnueli, Eds. Springer, 2003.

[4] B. Bose, "The past, present, and future of power electronics," *IEEE Industrial Electronics Magazine*, vol. 3, no. 2, pp. 7–11, 2009.

[5] J. Holtz, "Power Electronics-A Continuing Challenge," *IEEE Industrial Electronics Magazine*, vol. 5, no. 2, pp. 6–15, 2011.

[6] S. Kouro, M. Malinowski, K. Gopakumar, J. Pou, L. Franquelo, B. Wu, J. Rodríguez, M. A. Pérez, and J. Leon, "Recent Advances and Industrial Applications of Multilevel Converters," *IEEE Transactions on Industrial Electronics*, vol. 57, no. 8, pp. 2553–2580, 2010.

[7] J. Ragot, G. Mourot, and D. Maquin, "Parameter estimation of switching piecewise linear system," in *Proceedings 42nd IEEE Conference on Decision and Control 2003*, Maui, Hawaii, USA, Dec. 2003, pp. 5783–5788.

[8] L. Bako, K. Boukharouba, and S. Lecoeuche, "Recovering Piecewise Affine Maps by Sparse Optimization," in *Proceedings of the 16th IFAC Symposium on System Identification*, Brussels, Belgium, Jul. 2012, pp. 356–361.

[9] A. Bemporad, A. Garulli, S. Paoletti, and A. Vicino, "A bounded-error approach to piecewise affine system identification," *IEEE Transactions on Automatic Control*, vol. 50, no. 10, pp. 1567–1580, Oct. 2005.

[10] H. Ohlsson, L. Ljung, and S. Boyd, "Segmentation of ARX-models using sum-of-norms regularization," *Automatica*, vol. 46, no. 6, pp. 1107–1111, Jun. 2010.

[11] E. Cinquemani, R. Porreca, G. Ferrari-Trecate, and J. Lygeros, "Parameter identification for stochastic hybrid models of biological interaction networks," in *46th IEEE Conference on Decision and Control*, New Orleans, LA, USA, Dec. 2007, pp. 5180–5185.

[12] J. I. Yuz, J. Alfaro, J. Agüero, and G. C. Goodwin, "Identification of continuous-time state-space models from non-uniform fast-sampled data," *IET Control Theory and Applications*, vol. 5, no. 7, pp. 842–855, 2011.

[13] A. Feuer and G. Goodwin, *Sampling in digital signal processing and control.* Birkhäuser, 1996.

[14] R. H. Middleton and G. C. Goodwin, *Digital Control and Estimation: A Unified Approach*, ser. Prentice-Hall Information and System Sciences Series. Prentice Hall, May 1990.

[15] R. Shumway and D. Stoffer, *Time series analysis and its applications*, 2nd ed. Springer, 2006.

[16] K. Åström, *Introduction to stochastic control theory.* Academic Press, New York, 1970.

[17] P. E. Kloeden and E. Platen, *Numerical solution of stochastic differential equations.* Springer, 1999, corrected Third Printing.

[18] T. Geyer, G. Papafotiou, and M. Morari, "Hybrid Model Predictive Control of the Step-Down DC–DC Converter," *IEEE Transactions on Control Systems Technology*, vol. 16, no. 6, pp. 1112–1124, 2008.

[19] S. Almer, S. Mariethoz, and M. Morari, "Piecewise affine modeling and control of a step-up DC-DC converter," in *American Control Conference (ACC), 2010*, 2010, pp. 3299–3304.

[20] D. E. Quevedo, R. P. Aguilera, M. A. Pérez, P. Cortés, and R. Lizana, "Model Predictive Control of an AFE Rectifier With Dynamic References," *IEEE Transactions on Power Electronics*, vol. 27, no. 7, pp. 3128–3136, 2012.

[21] F. J. Bejarano, M. Ghanes, and J. P. Barbot, "Observability and observer design for hybrid multicell choppers," *International Journal of Control*, vol. 83, no. 3, pp. 617–632, Mar. 2010.

[22] A. P. Dempster, N. M. Laird, and D. B. Rubin, "Maximum likelihood from incomplete data via the EM algorithm," *Journal of the Royal Statistical Society. Series B*, vol. 39, no. 1, pp. 1–38, 1977.

[23] H. White, *Estimation, inference and specification analysis.* Cambridge University Press, 1996.

[24] J. C. Agüero, W. Tang, J. I. Yuz, R. Delgado, and G. C. Goodwin, "Dual-time frequency domain system identification," *Automatica*, vol. 48, no. 12, pp. 3031–3041, 2012.

[25] R. M. Neal and G. E. Hinton, *Learning in graphical models.* Kluwer Academic Publishers, 1998, ch. A view of the EM algorithm that justifies incremental, sparse, and other variants.

[26] G. C. Goodwin and J. C. Agüero, "Approximate EM algorithms for parameter and state estimation in nonlinear stochastic models," in *44th IEEE Conf. on Decision and Control and the European Control Conf. 2005*, Sevilla, Spain, 2005.

[27] B. I. Godoy, G. C. Goodwin, J. C. Agüero, D. Marelli, and T. Wigren, "On identification of FIR systems having quantized output data," *Automatica*, vol. 47, no. 9, pp. 1905–1915, 2011.

[28] O. Cappé, E. Moulines, and T. Rydén, *Inference in hidden Markov models*. Springer, 2005.

[29] S. Yang, D. Xiang, A. Bryant, P. Mawby, L. Ran, and P. P. E. I. T. o. Tavner, "Condition Monitoring for Device Reliability in Power Electronic Converters: A Review," *IEEE Transactions on Power Electronics*, vol. 25, no. 11, Nov. 2010.

[30] Y. Song and B. Wang, "Survey on Reliability of Power Electronic Systems," *IEEE Transactions on Power Electronics*, vol. 28, no. 1, pp. 591–604, Jan. 2013.

[31] P. Lezana, J. Pou, T. A. Meynard, J. Rodríguez, S. Ceballos, and F. Richardeau, "Survey on Fault Operation on Multilevel Inverters," *IEEE Transactions on Industrial Electronics*, vol. 57, no. 7, pp. 2207–2218, 2010.

[32] C. Turpin, P. Baudesson, F. Richardeau, F. Forest, and T. A. Meynard, "Fault management of multicell converters," *IEEE Transactions on Industrial Electronics*, vol. 49, no. 5, pp. 988–997, 2002.

[33] R. P. Aguilera, D. E. Quevedo, T. Summers, and P. Lezana, "Predictive control algorithm robustness for achieving fault tolerance in multicell converters," in *Industrial Electronics, 2008. IECON 2008. 34th Annual Conference of IEEE*, Nov. 2008, pp. 3302–3308.

[34] P. Lezana, R. Aguilera, and J. Rodríguez, "Fault Detection on Multicell Converter Based on Output Voltage Frequency Analysis," *IEEE Transactions on Industrial Electronics*, vol. 56, no. 6, pp. 2275–2283, 2009.

[35] G. M. Buiatti, J. Martin-Ramos, C. H. R. Garcia, A. M. R. Amaral, and A. J. Marques Cardoso, "An Online and Noninvasive Technique for the Condition Monitoring of Capacitors in Boost Converters," *IEEE Transactions on Instrumentation and Measurement*, vol. 59, no. 8, Aug. 2010.

[36] M. Ghanes, J. B. Barbot, J. De Leon, and A. Glumineau, "A robust sensorless output feedback controller of the induction motor drives: new design and experimental validation," *International Journal of Control*, vol. 83, no. 3, pp. 484–497, Mar. 2010.

[37] T. Boileau, N. Leboeuf, B. Nahid-Mobarakeh, and F. Meibody-Tabar, "Online Identification of PMSM Parameters: Parameter Identifiability and Estimator Comparative Study," *IEEE Transactions on Industry Applications*, vol. 47, no. 4, pp. 1944–1957, Jul. 2011.

[38] B. Vaseghi, N. Takorabet, and F. Meibody-Tabar, "Fault Analysis and Parameter Identification of Permanent-Magnet Motors by the Finite-Element Method," *IEEE Transactions on Magnetics*, vol. 45, no. 9, pp. 3290–3295, Sep. 2009.

[39] I. R. Pérez, J. C. Silva, E. J. Yuz, and R. G. Carrasco, "Experimental sensorless vector control performance of a DFIG based on an extended Kalman filter," in *38th IEEE Annual Conference on Industrial Electronics Society (IECON)*, 2012, pp. 1786–1792.

[40] T. A. Meynard, H. Foch, P. Thomas, J. Courault, R. Jakob, and M. Nahrstaedt, "Multi-cell converters: basic concepts and industry applications," *IEEE Transactions on Industrial Electronics*, vol. 49, no. 5, pp. 955–964, 2002.

[41] E. Silva, B. McGrath, D. E. Quevedo, and G. C. Goodwin, "Predictive Control of a Flying Capacitor Converter," in *American Control Conference, 2007. ACC '07*, 2007, pp. 3763–3768.

[42] P. Lezana, R. P. Aguilera, and D. E. Quevedo, "Model Predictive Control of an Asymmetric Flying Capacitor Converter," *IEEE Transactions on Industrial Electronics*, vol. 56, no. 6, pp. 1839–1846, 2009.

[43] D. Patino, M. Bâja, P. Riedinger, H. Cormerais, J. Buisson, and C. Iung, "Alternative control methods for DC-DC converters: An application to a four-level three-cell DC-DC converter," *International Journal of Robust and Nonlinear Control*, vol. 21, no. 10, pp. 1112–1133, Sep. 2010.

[44] G. C. Montanari and D. Fabiani, "Searching for the factors which affect self-healing capacitor degradation under non-sinusoidal voltage," *IEEE Transactions on Dielectrics and Electrical Insulation*, vol. 6, no. 3, pp. 319–325, Jun. 1999.

[45] R. P. Aguilera, P. Lezana, and D. E. Quevedo, "Finite-Control-Set Model Predictive Control With Improved Steady-State Performance," *IEEE Transactions on Industrial Informatics*, vol. 9, no. 2, pp. 658–667, May 2013.

[46] J. Yuz, J. Agüero, G. Goodwin, and J. Alfaro, "Connections between incremental and continuous-time EM algorithm for state space estimation," in *16th IFAC Symp. on System Identification*, 2012, pp. 834–839.

[47] A. Jazwinsky, *Stochastic processes and filtering theory*. Academic Press, San Diego, CA, 1970.

[48] B. Oksendal, *Stochastic differential equations: an introduction with applications*, 6th ed. Springer, 2003.

[49] K. Åström and B. Wittenmark, *Computer-Controlled Systems: Theory and design*, 2nd ed. Prentice-Hall, 1990.